Proceedings World Geothermal Congress 2020+1
Reykjavik, Iceland, April - October 2021

Coupled Production Facility and Geothermal Well Performance Modelling: Case Studies and Insights

Dale Emet Altar, Nigel Joseph Kabigting, Joy Cristine Tolentino and Miguel Enrico Villena

14th Floor 6750 Building, 6750 Ayala Avenue, Makati City, Metro Manila, Philippines

DAltar@pgpc.com.ph

Keywords: Tiwi, Mak-Ban, production, injection, well, fluid transport, gathering system, injection system, numerical model, multi-phase, flow simulator

ABSTRACT

Numerical modelling is an essential tool for the assessment of geothermal production facilities, for the evaluation of optimization opportunities, as well as for forecasting the future performance of a plant when change is introduced. In all these functions, numerical models support decision-making – be it for day-to-day response, or for strategy development.

For two-phase, intermediate enthalpy production systems like in the Tiwi and Mak-Ban geothermal fields in the Philippines, transport phenomena have significant impacts on the overall system production. Transport can account for 65% (as high as 80% in cases) of the overall pressure difference between production wells and the plants, with the remainder due to processes such as separation and scrubbing. This presents an opportunity for the optimization of transport facilities for better field performance.

Facilities Engineers in the Philippine Geothermal Production Company, Inc. (PGPC), which operate the Tiwi and Mak-Ban geothermal fields, have long utilized fluid transport facility numerical models in order to understand the process and to make strategic decisions. The earliest documented use of numerical modelling software in PGPC was in 1989 using PIPEFLOW, described as "an off shoot from the Tiwi pipeline network programs" (Wendt, 1989). Current softwares have certainly come a long way from PIPEFLOW, which was only capable of single pipeline calculations.

Commercially available transport modelling softwares primarily focus on steady-state network calculations. Steady state modelling is however limited in the analysis of established systems where processes can change as affected by process upsets, shutdowns, facility upgrades, or even the development of flow assurance issues. Analyses for these types of issues require the integration of well performance information. Accurate representation of geothermal wells leads to decisions that are better informed and closer to reality. This becomes especially important for high-capital decisions involving transport and pumping facilities.

This paper presents case studies on adapting commercially available steady-state transport modeling software for the integration of production or injection well performance data. It also documents the results of three case studies, results of the integrated analysis. One case study is the Tiwi WS-06 System Debottlenecking, where modeling indicated the presence of a major blockage in a steam line. The blockage was found and cleaned out, yielding a gain of 4 MWe. A second case history is the Mak-Ban Planned Shutdowns Contingency Planning, where modeling was used to plan for optimal re-routing of well flows in case of an extended shutdown of a steam separation station. A third case history is the Mak-Ban Hot Brine Injection System Optimization, wherein the model has supported cost, scope and schedule optimization of ongoing and future system improvements to ensure reliable brine injection capacity.

The integrated modeling approach allowed the project teams to fully quantify the effects of system optimization for two-phase production systems. It also supported the full accounting of system-wide brine injection capacity as affected by the inter-relation of network pressures and well injection capacity as affected by pump performance and flow assurance issues.

1. INTRODUCTION

The Philippine Geothermal Production Company, Inc. (PGPC) operates both the Tiwi and Mak-Ban Geothermal Fields in the Philippines. The Tiwi Geothermal Field, located in the province of Albay on the island of Luzon, has been in commercial production since 1979. It was the first geothermal field developed in the country. The Makiling-Banahaw (Mak-Ban) Geothermal Field located in the provinces of Batangas and Laguna has likewise been in production for 40 years.

In the past decade, Philippine Geothermal Production Company Inc. (PGPC) has focused its operations in the Mak-Ban and Tiwi geothermal fields on the optimization of existing production facilities and well capacities to ensure a stable and reliable geothermal steam supply to the power plants. Internal processes and projects are continuously identified, and implemented year after year in support of optimization. At the core of these efforts is PGPC's in-house capability of assessing and predicting overall system performance through production facilities numerical modelling.

Production facility modelling is being conducted using commercial softwares – with PipePhase by AVEVA (formerly SimSci), or FluidFlow by Flite Software NI Ltd. Most softwares at their core are steady-state, multi-phase fluid flow simulators. They are being used extensively in PGPC to analyze and predict the behavior of steam and two-phase piping networks—in the early phases of project development, as well as in system troubleshooting, and even in production planning.

However, steady-state calculations fail to capture inherent system variabilities arising from changing well deliverabilities and equipment performance. Adapting them for dynamic simulation allows for the creation of more robust models which better match field performance.

2. WELL DELIVERABILITIES AND INJECTIVITIES

The primary cause of the system's dynamic behavior are the production and injection wells. In the field, geothermal production wells respond inversely to surface facility pressures, reducing mass flow rate as the wellhead pressure increases, and vice versa. The addition of a new well, steam venting, or even the installation of an orifice meter all produce a pressure response in a fluid transport network, and thus elicit a corresponding response in wells connected to the network. It is therefore critical that before any dynamic modelling proceeds that production well behavior is appropriately represented.

One way to capture well behavior is to model from the reservoir, through the wellbore, into the surface facilities and PGPC is presently working to improve its ability to do this. Therefore, for the present modeling, well deliverability curves have been used to model the changes in well performance as a function of wellhead pressure as they are more directly measurable.

Well deliverability curves, also known as output curves, describe the behavior of mass flow with flowing wellhead pressure (FWHP). In principle, the shape of a curve is influenced by several factors such as reservoir pressure, feed enthalpies, and wellbore completion. Figure 1 shows different output curves resulting from different well and reservoir characteristics, assuming that neither enthalpy nor gas content of the wells vary significantly with WHP (Grant and Bixley, 2011). These assumptions were also applied in integrating deliverability curves in the steady state transport models.

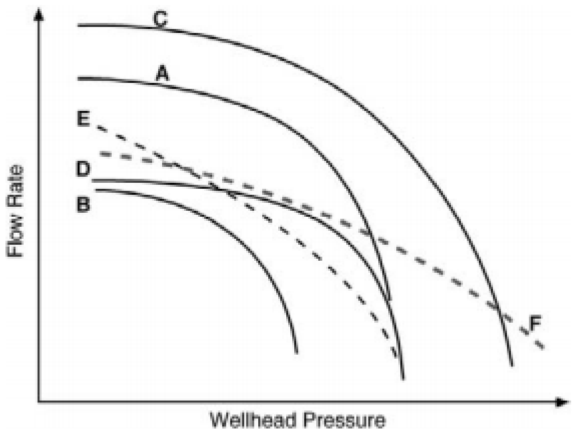

Figure 1: Variations of output curves showing (A) typical deliverability curve from a water-fed well of high permeability, (B) effect of decline in reservoir pressure, (C) effect of rise in reservoir pressure, (D) effect of scaling in wellbore, (E) effect of lower permeability, (F) well with two-phase feed at the same pressure as A. Reprinted from Grant & Bixley (2011).

Data on enthalpy variations for seven Mak-Ban Field wells are presented in Figure 2. Typically, dry steam wells more clearly demonstrate the constant enthalpy behavior over a range of pressures, e.g. BUL-113 and BUL-001. On the other hand, there is more spread in enthalpy data for two-phase wells. However, based on the data in Figure 2, the constant enthalpy behavior assumption is still reasonable even for two-phase wells as in both Tiwi and Mak-Ban, these wells are generally producing from liquid dominated feed zones.

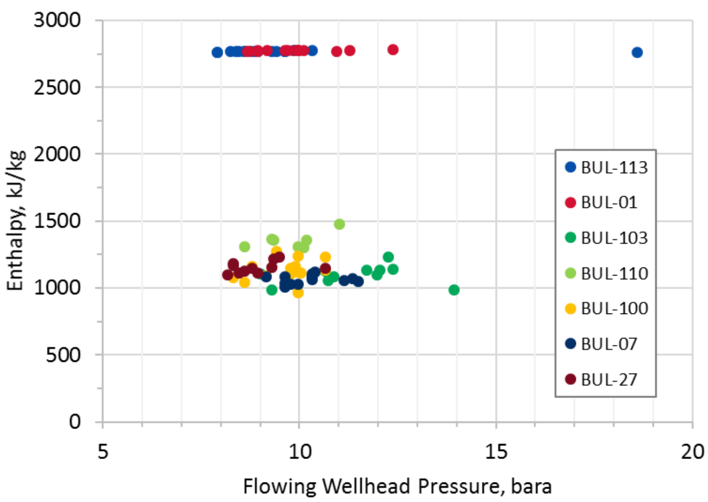

Figure 2: Flowing Wellhead Pressure versus Flowing Enthalpy Data for sample wells in the Mak-Ban Field.

Well deliverability curves are reported in PGPC in terms of steam rate, governed by a linear parabolic fit equation as seen in Equation 1.

$$q_{steam} = s\sqrt{MDP - WHP} \tag{1}$$

In Equation 1, q_{steam}, s, MDP and WHP are mass flow rate of steam, slope constant, maximum discharge pressure and flowing wellhead pressure, respectively. For the deliverability curve to be usable for transport models, the calculated steam rates are converted to total mass flow using the flowing enthalpy of each well. Deliverability curves for the same set of wells in Figure 2 are shown in Figure 3, plotted against the most recent tracer flow test (TFT) data for each well.

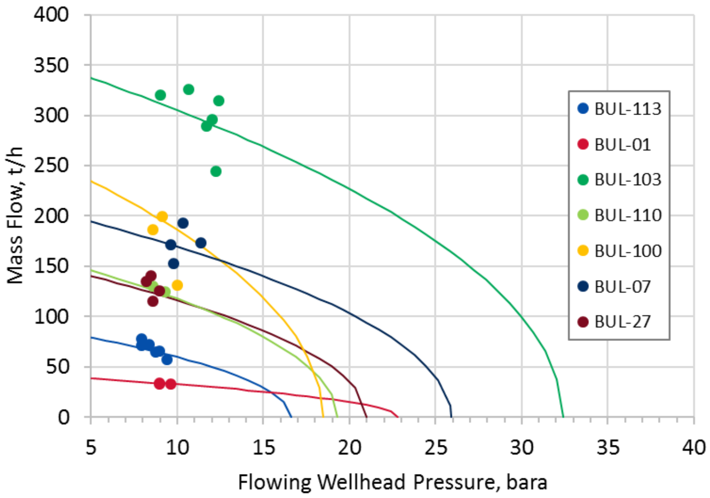

Figure 3: Flowing Wellhead Pressure versus Total Mass Flow Data and well deliverability curves for sample wells in the Mak-Ban Field.

For injection wells, well injectivities are affected by injection temperature. A decrease in injectivity is commonly observed with increasing fluid temperature (Siega et al., 2014). However, in the case of the Tiwi and Mak-Ban fields, separation pressures are normally maintained within 6 to 7.9 barg, corresponding to a maximum temperature variation of only 9.7 °C. Minimal changes to the fluid temperatures are also expected from piping heat loss (except when there is rainfall), so for simplicity, it is reasonable to assume that only injection pressure has a significant effect on the injection rate for each well.

For hot brine reinjection wells, injectivity curves are characteristically linear, provided that the injection pressure is above the saturation pressure corresponding to the injection temperature. Each incremental increase in injection pressure effects a proportional response in injection rate. This is illustrated in Figure 4.

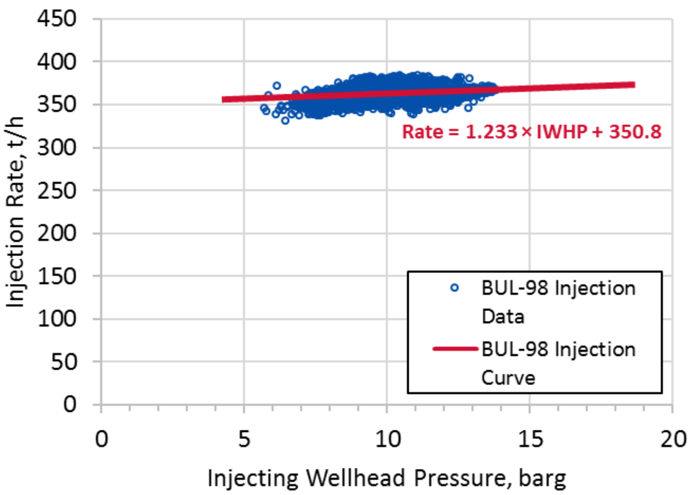

Figure 4: Injectivity curve for BUL-98 in hot brine service.

The injectivity equation is reported in the form

$$q_{brine} = s * IWHP + b \tag{2}$$

where q_{brine}, s, $IWHP$ and b are mass injection rate of brine, slope constant, injecting wellhead pressure and intercept, respectively.

In contrast, condensate and cold brine injectivity curves are defined as two distinct functions: a vertical linear function, for which the injection rate can range from 0 t/h to the minimum value wherein the wellbore is full; and a sloped linear function, similar to hot brine wells. It is important to note that the pressure value where the injection behavior changes corresponds to the saturation pressure for the injection temperature. This is observed in Figure 5 where the injectivity behavior changes at -0.875 barg.

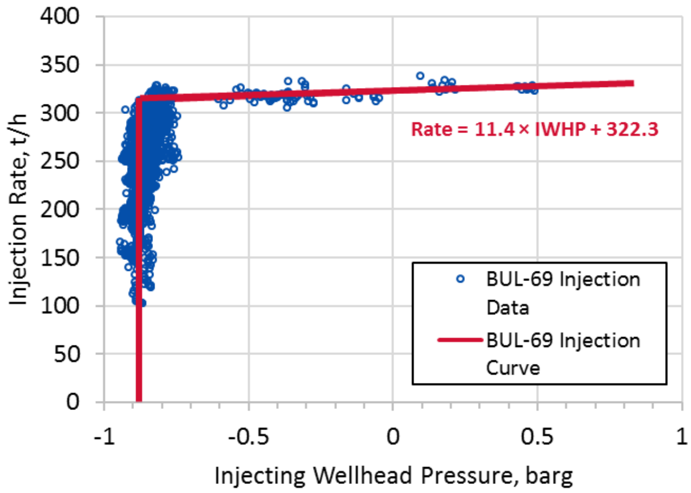

Figure 5: Injectivity curve for BUL-69 in condensate and cold brine service.

It is important to note that this dual behavior is not limited to condensate wells; hot brine reinjectors also exhibit this behavior at lower injection rates, where the wellhead pressure may be below the saturation pressure corresponding to the reinjection temperature. However, most hot brine reinjectors are maximized and not operated below the saturation pressure because such an operation mode increases the scaling risk for wells.

3. METHODOLOGY

Different software packages offer different solutions for the integration of well performance curves. The method of integration is also dependent on the calculation methods inherent to the software.

3.1 PipePhase

PipePhase offers an integration solution with Excel. This direct interface between the two software allows for the creation of macro-enabled spreadsheets that are linked to the process model. From Excel, the user can command the model to run, as well as to enter calculations directly as model boundary inputs. In this case, Equation 1 was used with well enthalpy to get the total mass flow as mass input to model source nodes. An iterative method was implemented, with well flowrates and steam qualities recalculated based on the model pressures at the end of each model run. The new values are then used for the next iteration, and the process is repeated until a final steady state is reached. The iterative methodology flowchart is presented in Figure 6. The pressure results at each iteration for a sample model are shown in Figure 7.

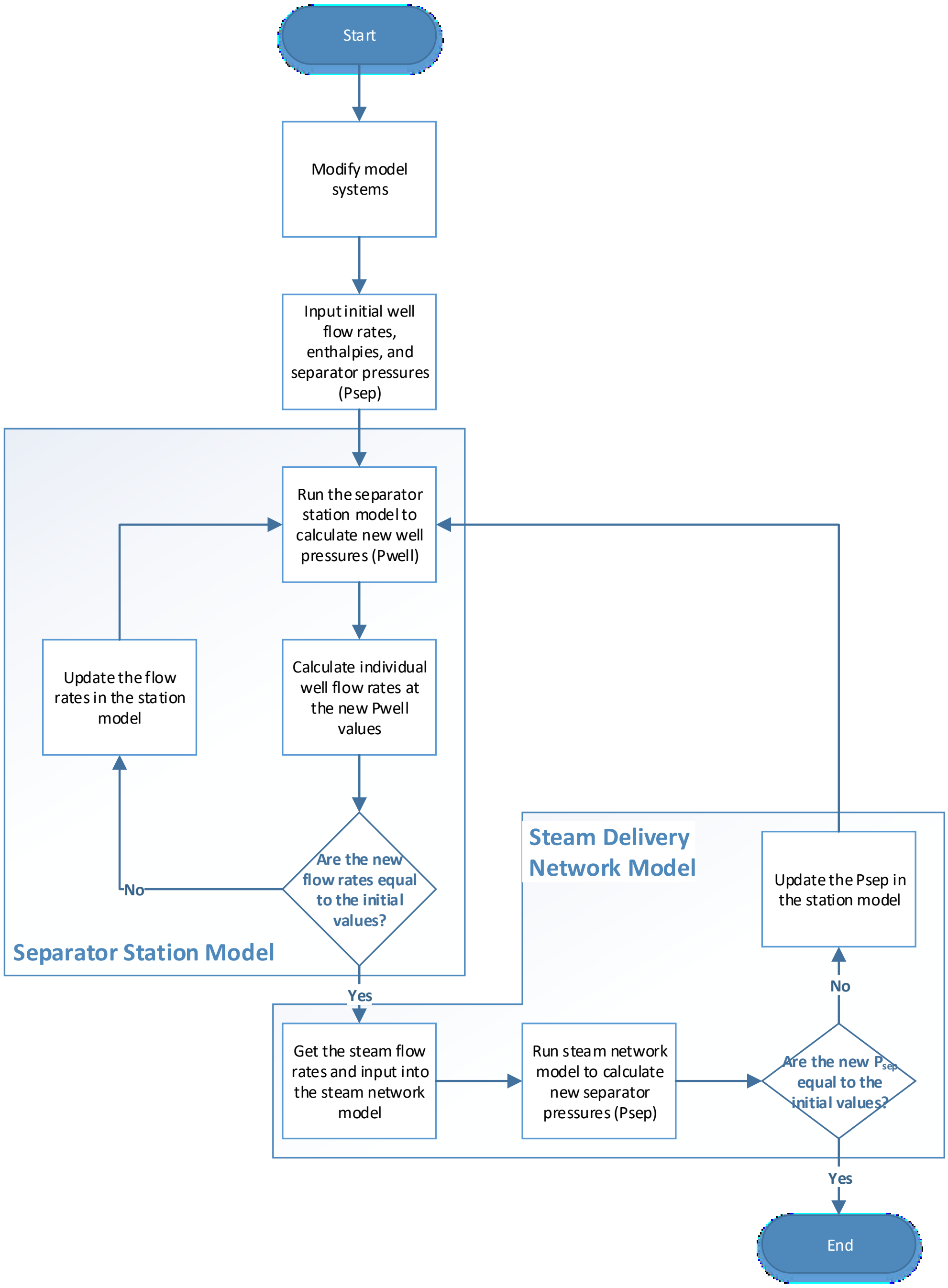

Figure 6: Iterative solution flowchart for the integration of well productivities in production facility models.

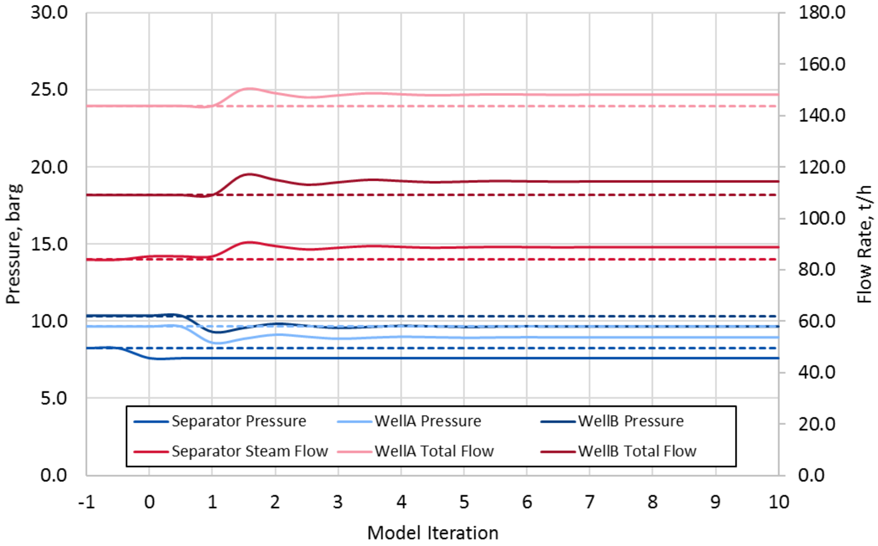

Figure 7: Two-phase model response to a change in separation pressure for each model iteration. Dotted lines indicate original state for comparison, while zero position indicates the point of change introduction from a steady state.

The methodology can be executed manually from the modelling software, with the exception of well production calculations, which are done via Excel. The use of the integration solution allowed for the automation of the process from a single interface, significantly cutting analysis time. Separation Stations are also modelled separately from the Steam Delivery Network to manage model sizes. The Excel integration connected the two models via the separator vessel parameters and cell references, and allowed the user to run the models one after the other with each iteration, something that is otherwise impossible to do directly from the software. A sample sheet from a linked Excel workbook is shown in Figure 8.

Wellsite Production Data	**WS-06**					
	Slope	MDP	Wmax of stea	Enthalpy, kJ/k	Quality at Constant Enthalpy	
KAP22	15.1	29	59	1221	19.5	%
KAP21	18.7	33	80	1133	14.0	%
KAP20	19.6	19	48	1068	11.9	%
KAP35	43.8	24	130	1191	16.9	%
KAP22:Weight Flow Rate	257.4	t/h				
KAP22:Pressure	13.7	barg				
KAP22:Vapor Quality (wt)	19.5					
KAP21:Weight Flow Rate	501.8	t/h				
KAP21:Pressure	15.2	barg				
KAP21:Vapor Quality (wt)	14.0					
KAP20:Weight Flow Rate	291.8	t/h				
KAP20:Pressure	13.4	barg				
KAP20:Vapor Quality (wt)	11.9					
KAP35:Weight Flow Rate	609.8	t/h				
KAP35:Pressure	15.4	barg				
KAP35:Vapor Quality (wt)	16.9					

Figure 8: Sample sheet from a linked Excel workbook. Cells highlighted by the red box are linked to the model.

3.2 FluidFlow

Inclusion of production well performance in FluidFlow was executed differently based on the principle of isenthalpic flash. When two-phase fluids or saturated liquids encounter a flow device along its path that induces a pressure drop with no heat loss, e.g. a throttling valve, the fluid enthalpy is conserved. However, the fluid re-equilibriates at the lower pressure conditions, which translates to an increase in the vapor phase and an equivalent decrease in the liquid phase. The final fluid quality is related to the inlet enthalpy via Equation 3.

$$x = \frac{h_{f1} - h_{l2}}{h_{v2} - h_{l2}} \tag{3}$$

In Equation 3, x, h_{f1}, h_{l2} and h_{v2} are steam quality, fluid enthalpy at the upstream condition, saturated liquid enthalpy at the downstream pressure, and saturated vapor enthalpy at the downstream pressure.

The FluidFlow software includes a *User Defined Generic* (UDG), a unit which allows the user to input custom functions relating fluid flow rate to pressure drop following the general form

$$\Delta P = K + ABQ^n + CDQ^m \tag{4}$$

where *ΔP* and *Q* are pressure drop and flow rate (either volumetric or mass) respectively, while *A*, *B*, *C*, *D*, *n* and *m* are equation constants. To model each individual well, a combination of a UDG and a fixed pressure node unit are used. This is illustrated in Figure 9, highlighted in the red box.

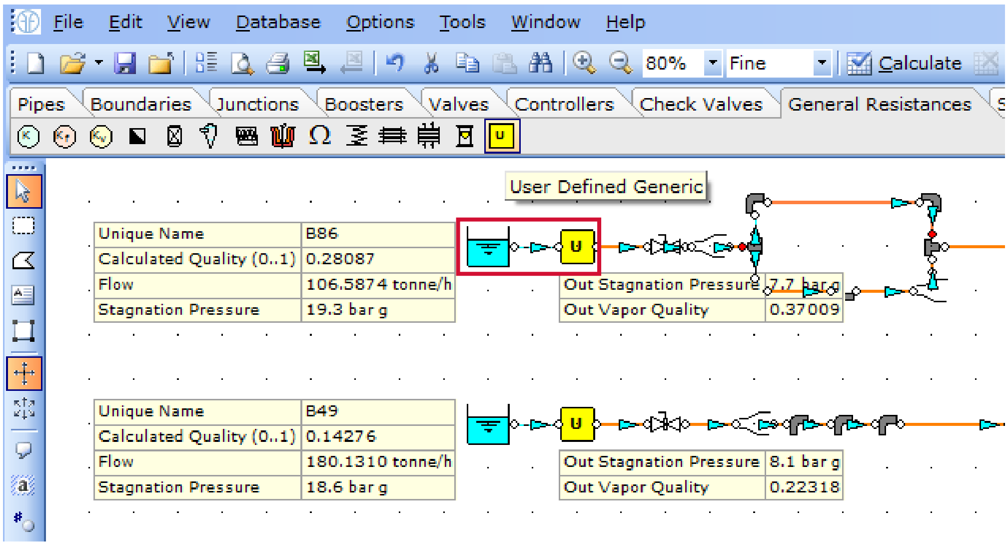

Figure 9: Sample production well model, indicated by the red box.

First, *MDP* for the well is set as the boundary condition for the fixed pressure node, along with the steam quality that corresponds to the well's enthalpy at the *MDP*. The UDG is then used as a flash device, producing a pressure drop response such that the pressure downstream of the UDG corresponds to the well's *WHP*. FluidFlow automatically runs the flash calculation (Equation 3), giving the steam quality at the *WHP*. The relationship between the *MDP*, *WHP* and ΔP_{UDG}, the pressure drop across the UDG is given by

$$WHP = MDP - \Delta P_{UDG} \tag{5}$$

The equation for the UDG is based on fitting a second-order polynomial on the well production data versus the ΔP_{UDG} derived from Equation 5. Generally, the resulting curve follows the general form

$$\Delta P_{UDG} = c * q_{total}{}^2 \tag{6}$$

where *c* and q_{total} are the equation constant and the total production mass rate of each well, respectively.

A similar approach is carried out for hot brine injection wells, but with the fixed pressure node located downstream of the UDG, set at a pressure of 0 barg. This simplifies the UDG equation as the ΔP_{UDG} is then equivalent to the injecting wellhead pressure for a given injection rate. Replacing the *IWHP* term in Equation 2 with the ΔP_{UDG} and rearranging gives the UDG equation for hot brine wells as

$$\Delta P_{UDG} = \frac{q_{brine}}{s} - \frac{b}{s} \tag{7}$$

There is however an additional modification imposed on the UDG behavior. Due to the pressure drop to 0 barg, the high temperature brine will flash across the UDG. To prevent this, a fixed temperature loss is imposed on the brine at the UDG such that the final fluid temperature will be below 100 °C.

For condensate and cold brine wells, the fixed pressure node is set at a pressure 2% higher than the saturation pressure at the reinjection temperature, the minimum injection pressure (*MIP*). This is done for two reasons: it ensures that the injectate will not flash across the UDG while closely approximating injection at saturation pressure, and it simplifies switching between the full wellbore injection behavior and the static injection pressure behavior. For the static injection pressure behavior, the UDG is simply set to be ignored by the model, such that the *MIP* is used as the injection pressure, while for the full wellbore behavior, the UDG is set as active. The equation for the UDG is

$$\Delta P_{UDG} = \frac{q_{brine}}{s} - \frac{(b+MIP)}{s} \tag{8}$$

The same approach for condensate wells can be applied for hot brine wells if the engineer wishes to capture the system performance when injecting at flashing conditions. An example of a well modelled to be injecting at saturation pressure is shown in Figure 10. Note that the broken lines around the highlighted UDG indicate that it is inactive, and thus, will not produce a pressure drop with flow.

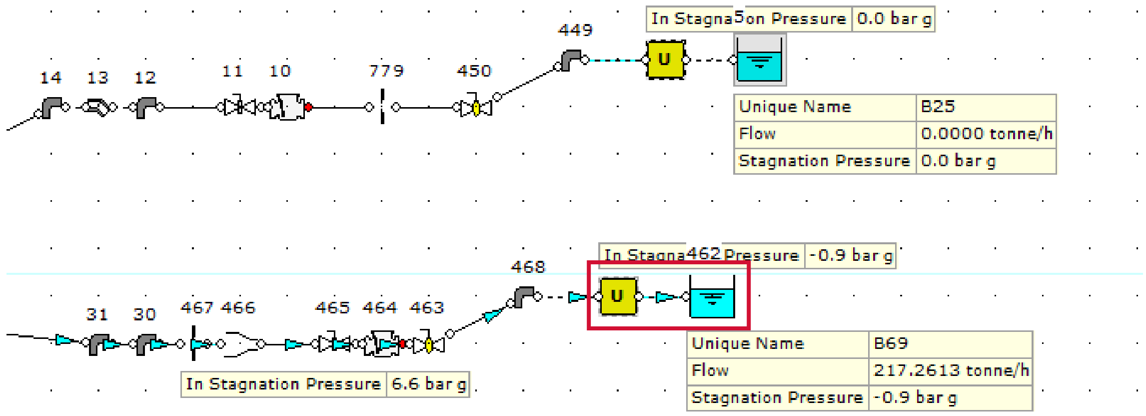

Figure 10: Sample condensate well model, indicated by the red box.

Once these parameters are set, FluidFlow calculates the output from the UDGs as part of its solution, removing the need for any iterative methodology on the part of the modeler.

4. CASE STUDIES

The following case studies illustrate the application of these modelling methods to specific production and brine disposal challenges. Decisions and outcomes from modelling recommendations are also presented.

4.1 Tiwi WS-06 System Debottlenecking

At the start of 2014, Plant Station C in Tiwi was generating an average of 110 MWe. By October of the same year, the generation was down to 102 MWe (~8% decline). Monitoring reports showed that parts of the system were experiencing significant pressure drops along the piping network (both the two-phase and steam delivery networks), affecting well productivity such that there was an opportunity to gain incremental steam from system pressure reduction, or debottlenecking.

Before an assessment of the effect of system debottlenecking was carried out, process models were compared against system behavior. Figure 11 shows the results of the system model for WS-06 in Tiwi, in terms of modelled steam production at various separation pressures, plotted against actual steam measurements.

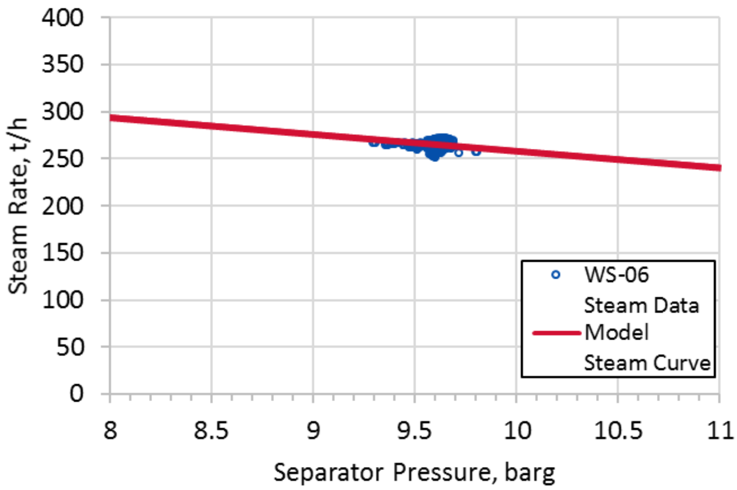

Figure 11: Modelled steam production of WS-06 in 2014 using production well curves versus measured data.

WS-06 is a wellpad-based separation station serving four wells. At the time of the project, WS-06 operated at a separation pressure of 140 psig (9.7 barg) producing 580 kph (264 t/h) of steam. Modelling showed that the separation pressure should only be at 115 psig (7.9 barg) for its steam production (as shown in Figure 12), and it indicated that the high pressure drop was occurring along the steam line from WS-06 going into the cross-country line. To match actual behavior, a choke orifice needed to be placed along the line in the model.

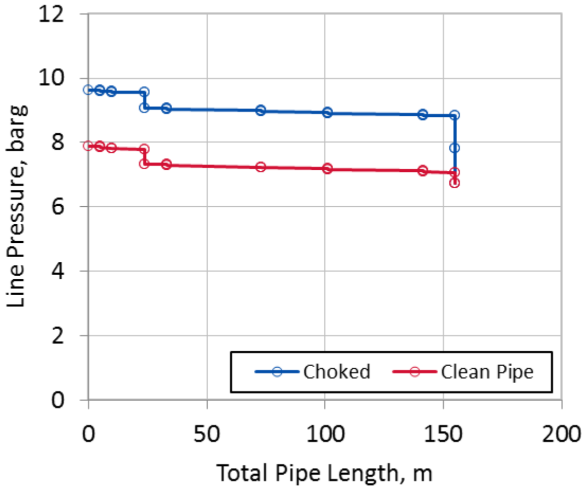

Figure 12: Modelled WS-06 steam line pressure profiles at choked and clean pipe conditions; zero length denotes the separator steam outlet.

Historical analysis of its separator pressure versus steam production showed counter-intuitive behavior; whereas the steam rate is decreasing after an initial period of high production, the separator pressure followed a continuous uptrend as presented in Figure 13.

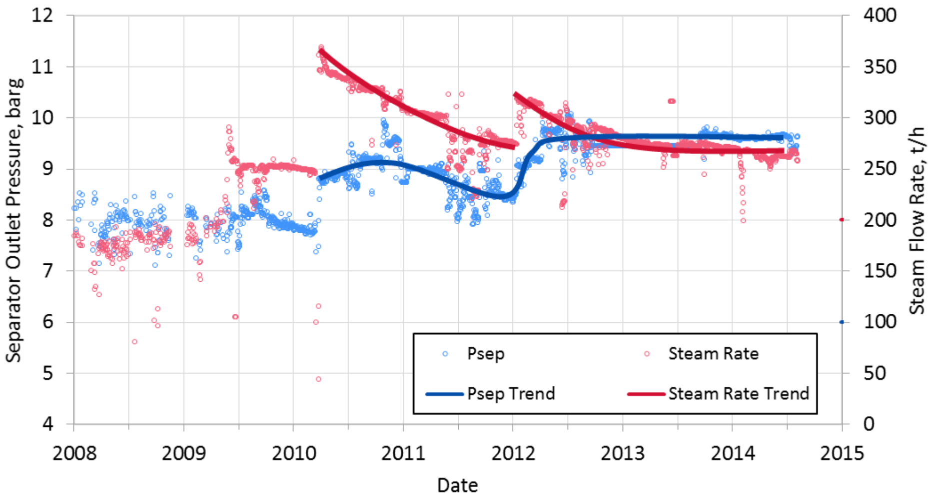

Figure 13: Historical production and separator pressure (P_{sep}) for WS-06 showing data trends.

The initial period of high production was due to the hook-up of a new well. After its flowing, frequent high level events were experienced at the WS-06 Separator, with brine from the new well fluctuating from 800 kph (360 t/h) to 1500 kph (680 t/h), leading the team to suspect brine carryover and scale formation along the steam line. However, in the period considered, no brine carryover events were observed at the plant station as the steam quality is further improved with a steam scrubber upstream of the turbine units.

To ascertain the presence and location of a choke point, pressure mapping was conducted. Based on the pressure mapping, the choke point was located at an elbow immediately upstream of the WS-06 steam line tie-in to the cross-country network. Prior to any decision to shutdown the system to address the issue, the model was re-run with the latest well productivity curves to quantify the benefits versus the associated losses. It was found that the net decrease in pressure of 25 psi (1.7 bar) expected after removing the blockage translates to 67 kph (30.5 t/h) of incremental steam gain (~3.7 MWe at 8.2 t/h/MWe) and 60 kph (27.3 t/h) additional brine, distributed among the four wells in WS-06.

PGPC management made the decision in 2015 to shutdown WS-06, a year in advance of its scheduled wellsite turnaround date, to inspect the line based on the model results and opportunity economics. During inspection, the presence of silica scales along the steam line was visually confirmed (Figure 14). The Tiwi Operations team then proceeded to replace the affected sections of the steam line. Upon recommissioning the system, the separation pressure at WS-06 went down to the expected value of 115psig (7.9 barg), with a net gain at the power station of 4 MWe,

Figure 14: Scale blockage observed within the WS-06 steam line in 2015.

4.2 Mak-Ban Hot Brine Injection System Optimization

The Mak-Ban Field Hot Brine Injection System (HBIS) is a brine disposal network serving eight separation stations, i.e. Satellite Stations (SS) 1 to 7, and 1B, with over 25 kilometers of pipeline ranging in size from 12 inches to 18 inches. Brine from each station is pumped into the network and transported to 11 hot brine injector wells. HBIS is facing capacity issues manifested through frequent opening of separator Emergency Dump Valves (EDV) at multiple stations. The dumped hot brine flows to sumps and is eventually injected as cold brine.

Many possible causes of the capacity issues such as higher brine production, lower pump performance, network congestion, and lower injection well capacities were considered. However, without a means of understanding the system as a whole and the interplay the system's components have with each other, the exact problem was difficult to identify. Understanding how each component of the system behaves individually and how each affects another in the system became the first step towards solving the issue. Modelling software is the most appropriate tool to represent the HBIS and its components and to simulate multiple scenarios to see how the system performs overall.

Building the model heavily relied on process information such as drawings, pressure and flow data, and historical equipment performance data. The availability of field data is critical to properly calibrate the model such that it could replicate conditions as observed in the field.

Upon calibration of the model, issues in the system were revealed. Calibration adjustments to allow the model to perform as observed in the field narrowed the search for the root causes of the issues. Examples of these adjustments include the reduction of line flow areas in certain locations where observed differential pressures were higher than calculated by the model (Figure 15), and scaling down performance curves for the operating pumps across the system following affinity laws based on the field data.

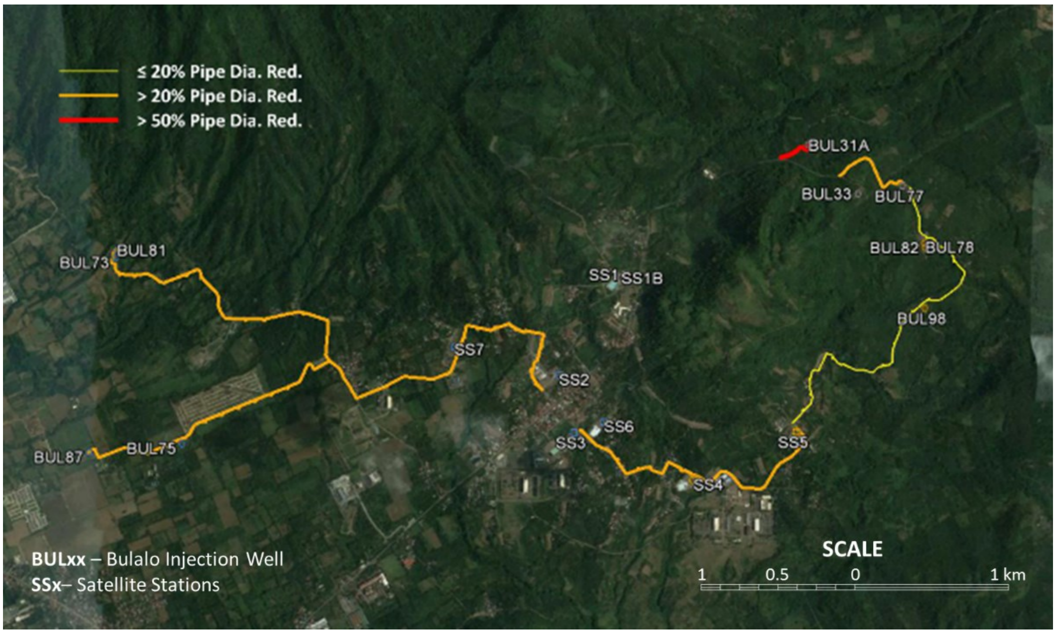

Figure 15: HBIS network sections with scale build-up, color coded based on percentage of pipe diameter occupied by scale.

From the calibration and model runs, one conclusion drawn was that sections of the network have reduced capacity due to the build-up of silica scale as indicated by the higher pressure drops along them. Injection pumps along the network have also become inadequate against requirements due to the higher discharge pressures needed to successfully inject the higher brine production from the field. A historical comparison of brine production versus discharge capacity per satellite station is shown in Figure 16. Lastly, more injectors are needed to handle both existing and future brine production to keep the system operating within its current pressure rating constraints.

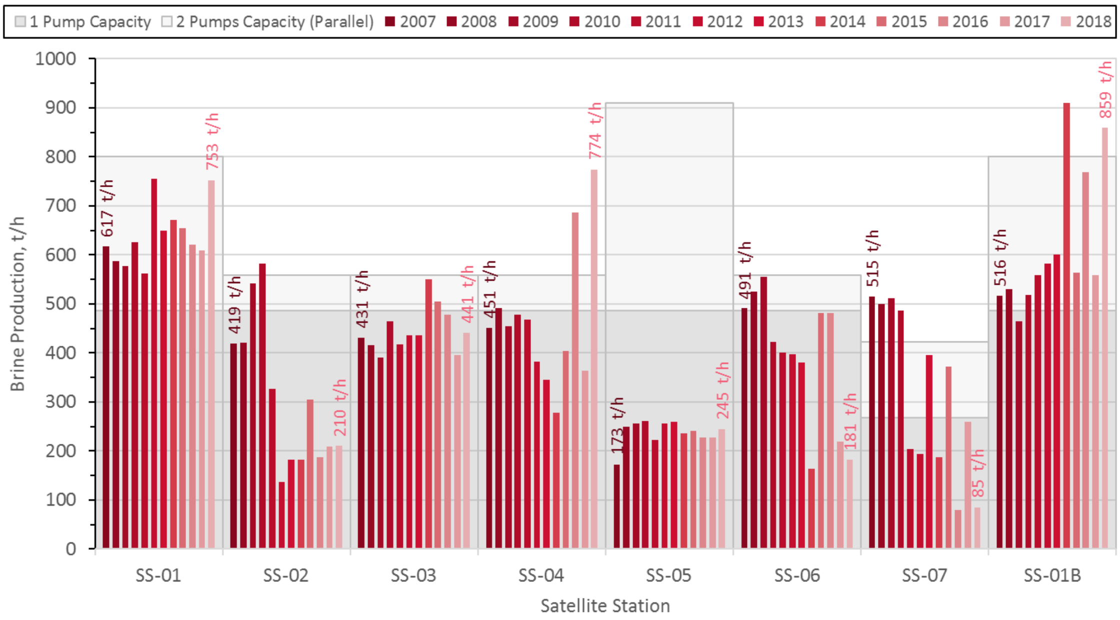

Figure 16: Historical hot brine production against pump capacity per satellite station. Single pump capacities are reported based on rated values, while two pump capacities are reported in relation to the required system pressures at the respective satellite stations for parallel pump operation.

Short and long term plans were set out based on the results of the analysis. For the determined HBIS line restrictions, inspections were conducted to validate the findings, during which silica scaling was confirmed. In the long term, new twin parallel lines along the determined restricted segments will be constructed to support the drilling of new wells. For the under-capacity pumps, new pumps of higher discharge capacities will be purchased and installed. Idle injectors are also being recommissioned to augment capacity as a temporary measure, while new multi-lateral injectors are planned for drilling in the next two years. In all identified solutions, the overall system response, including injector response, was accounted for in order to generate realistic solutions and predict reasonable outcomes. Figure 17 shows both the current network pressure profiles and the expected profile upon completion of recommendations.

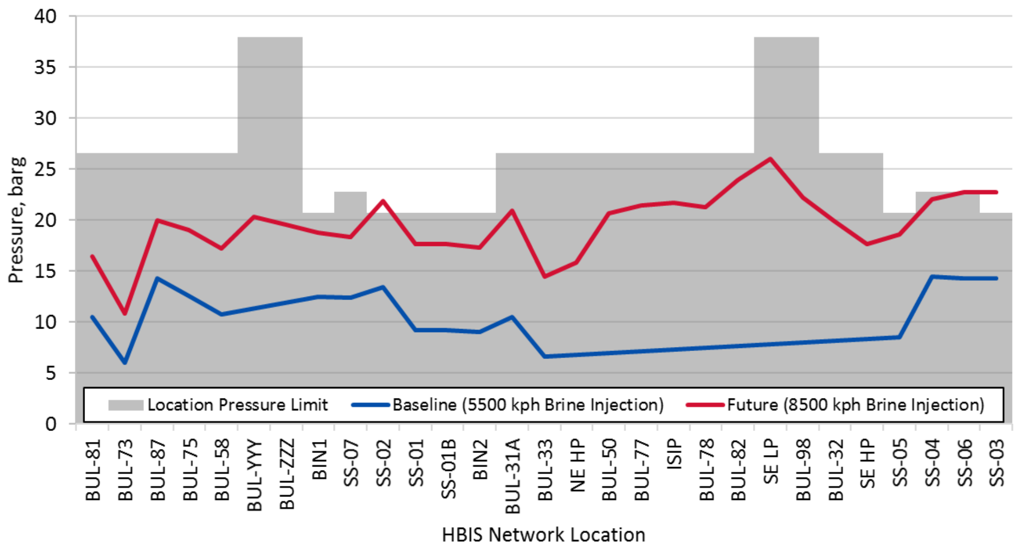

Figure 17: Comparative plot of current network pressure profile and modelled future network performance.

4.3 Mak-Ban Planned Shutdowns Contingency Planning

Separation stations in both the Mak-Ban and Tiwi fields are shut down every five years in order to conduct equipment maintenance. Each planned shutdown requires shutting in wells to de-energize the system, leading to production losses. As part of shut down planning, contingency strategies are put in place should there be a change in the shut down plan. One major risk considered is the extension of the shut down due to vessel inspection findings, for example, the identification of vessel weld failures. These types of issues cannot be addressed easily in the field, causing significant downtime.

One way to manage system losses for extended shut downs is to divert wells from the non-operating separation station to another, and in Mak-Ban, many wells are connected to two separation stations, facilitating well diversion. One specific case of this type of contingency planning was implemented for SS-07 in Mak-Ban in 2016. In the event of an extended shutdown of SS-07 (or in case of other failures for which SS-07 cannot be operated), the field will lose ~20MWe of generation. Two of the wells, BUL-23 and BUL-42, were not readily divertible due to the condition of their diversion line. One well, BUL-88 may be diverted to SS-01, but will incur significant losses due to back-pressure, though it utilizes a 24” line going to SS-07 with a connection to SS-02 that was isolated with a blind. Finally, there was an added requirement not to shut-in either BUL-66 or BUL-23 for well-specific issues.

The team looked at the option of diverting the entire production of SS-07 to SS-02 and SS-01 using all available swing lines between the stations, and determined the expected system and well pressures. An existing model of the two-phase production network with integrated well production curves was used. A section of the model is shown in Figure 18, with all available swing lines between SS-07 and SS-02 highlighted in red.

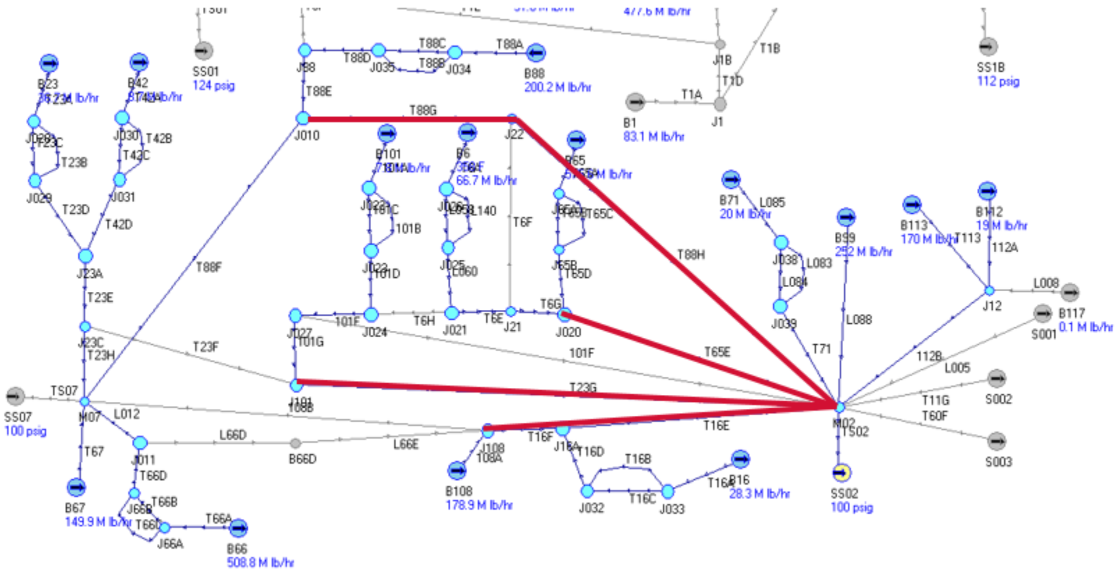

Figure 18: Two-phase production network model for SS-07 and SS-02 showing the available swing lines in red.

Back in March 2016, the three satellite stations produced a total of 85 MWe of steam. The model of the diversion strategy showed that increases in wellhead pressures in the connected wells of 2 psi (0.14 bar) to 42 psi (2.9 bar) were expected, along with an increase in the separation pressures at SS-01 and SS-02 of 11 psi (0.76 bar). A comparative plot of the initial and diversion pressures, as well as the mass rates for each well are shown in Figure 19. Modelling indicated that there are associated changes in mass flow rates for the calculated changes in pressure, and they all translate to a total steam loss of 88 kph (40 t/h). However, SS-01 and SS-02 feed steam to a plant with higher conversion efficiency such that despite the net loss of mass, only 2.5 MWe of power was expected to be lost due to the diversion compared to the base case.

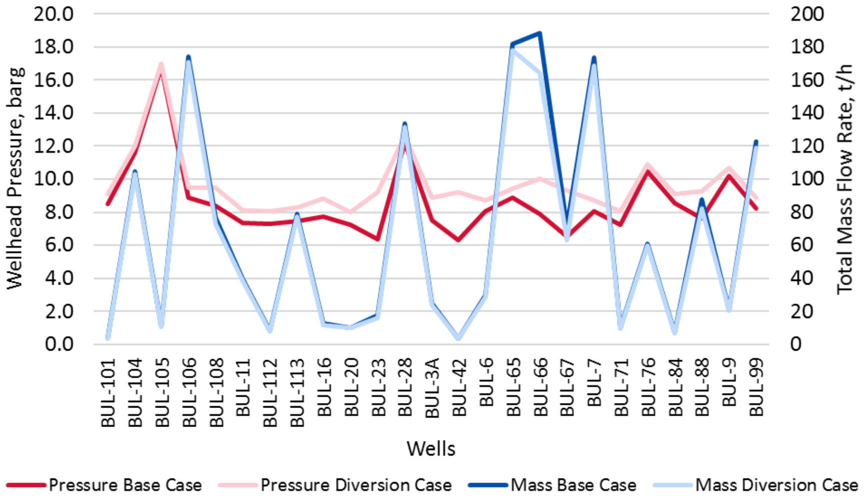

Figure 19: Comparative plot of well production parameters for the base and diversion cases.

The diversion contingency was endorsed by PGPC decision makers based on the results of the study, though it was ultimately not implemented as there were no major findings from the equipment inspections. The exercise did show the value of diversion case process modelling, and this form of contingency planning has been conducted for planned shutdowns and major unplanned shutdowns from 2016 to present.

5. SUMMARY AND RECOMMENDATIONS

The methodologies detailed in this paper provide practical guidance on integrating well performance into process models without the need for detailed well modelling. Incorporating well performance curves in production network models allows them to generate realistic results, giving project managers, operators and decision makers more confidence to proceed with system changes.

Numerical process modelling, if properly done, can help in understanding the current process, in identifying potential optimization opportunities, and provide insight on future process scenarios. The case studies presented show how transport network modelling aids in system troubleshooting, solutions identification, optimization and contingency planning.

REFERENCES

Grant, M. A., & Bixley, P. F.: Geothermal Reservoir Engineering (2nd ed.), (2011), US: Academic Press.

Siega, C., Grant, M., Bixley, P., & Mannington, W: Quantifying the Effect of Temperature on Well Injectivity, *Proceedings*, 36th New Zealand Geothermal Workshop, New Zealand (2014).

Wendt, B.: Follow-up on the Matalibong Crossover HAZOP Study Recommendation No. 3 - Heat Loss Calculations, (1989).